Title
Structure-Sensitive CO2 Electroreduction to Hydrocarbons on Ultrathin 5-fold Twinned Copper Nanowires

Authors
Li, Yifan
Cui, Fan
Ross, Michael B
et al.

Peer reviewed

Structure-dependent, selective electrochemical CO_2 conversion to methane on five-fold twinned copper nanowires

Yifan Li[1,†], Fan Cui[†], Michael B. Ross[#], Dohyung Kim, Yuchun Sun, Peidong Yang

[1] Department of Chemistry, University of California, Berkeley, CA 94720, USA

[2] Department of Materials Science and Engineering, University of California, Berkeley, CA 94720, USA

[3] Materials Sciences Division, Lawrence Berkeley National Laboratory, Berkeley, CA 94720, USA

[4] Kavli Energy Nanosciences Institute, Berkeley, CA 94720, USA

[†] These authors contributed equally to this work.

[*] To whom correspondence should be addressed. Email: p_yang@berkeley.edu

Copper is uniquely selective for the electrocatalytic reduction of carbon dioxide (CO_2) to products beyond carbon monoxide, such as methane (CH_4) and ethylene (C_2H_4). Therefore, understanding selectivity trends for CO_2 electrocatalysis on copper surfaces is a critical step towards developing more efficient catalysts for CO_2 conversion to higher order products. We investigated the electrocatalytic activity of ultrathin (<20 nm) five-fold twinned copper nanowires (Cu NWs) with a high density of twin boundary edge sites for CO_2 reduction. These Cu NW catalysts exhibited high CH_4 selectivity over other carbon products at high bias, reaching 55% Faradaic efficiency (F.E.) at -1.25 V vs. RHE while other products were produced with less than 5% F.E. Tracing the electrocatalytic activity as increasing charge is passed reveals that the selectivity for CH_4 gradually shifts towards producing C_2H_4, resulting in a 10% F.E. shift after 5 C passed. Simultaneously, the Cu NWs are observed to morphologically evolve, losing edge features in favor of forming small Cu nanoparticles. To prevent this structural change, the same Cu NW catalyst was wrapped with graphene oxide and *in situ* electrochemically reduced to a reduced graphene oxide wrapped copper nanowire (rGO-Cu NW) catalyst. Over the same period of charge passed, the rGO-Cu NW catalyst exhibits no observable morphological evolution, and simultaneously maintains high CH_4 selectivity without onset of C_2H_4 production. Our results suggest that CH_4 selectivity on Cu NWs is highly dependent on morphological features such as edge sites, and that hydrocarbon selectivity can be manipulated by structural evolution or the prevention thereof.

TOC graphic:

Electrocatalytic CO_2 conversion to value-added products is an attractive avenue to mitigating the unsustainable rise in anthropogenic CO_2 emissions. Coupled with renewably-generated electricity, such a system provides simultaneous carbon fixation and renewable energy storage.[1–3] Many catalytic studies in recent years have refined the electrocatalytic conversion of CO_2 to CO, increasing its viability by reducing overpotential and increasing current density.[4–9] On the other hand, an efficient electrocatalyst for the conversion of CO_2 to higher order products beyond CO has yet to be developed. Though several metals and metal alloys are known to produce small quantities of higher order products at high bias,[10] only copper has been shown to do so with appreciable activity.[11] Thus, copper is a suitable model material for the design of electrocatalysts that efficiently reduce CO_2 to higher order products. However, bulk polycrystalline copper foil produces a wide spread of products.[12,13] In addition, previous work has shown that the product distribution can be substantially influenced by various cleaning or surface treatment techniques.[14] Therefore, understanding how to manipulate selectivity on the copper surface, especially on the nanoscale, is critical for the development of new selective catalysts.

Nanoscale catalysts present considerable advantages to their bulk counterparts, including high surface area and a high density of low-coordination, high-activity catalytic sites. The enhancement of activity due to nanostructuring has been demonstrated for multiple catalytic materials, by improving turnover (i.e. partial current density towards products) and/or selectivity

at lower overpotentials.[5,6,15,8] Several different nanostructured copper catalysts have been investigated for aqueous CO_2 electrocatalysis to higher order products. Typically, the nanostructured catalyst films are produced through chemical and electrochemical treatments of copper foil, resulting in drastically improved selectivity and activity for high-value products like ethylene.[16–20] However, one downside is that the nanostructure and uniformity of the resulting electrodes is not well controlled. Colloidal nanomaterial synthesis provides the advantage of fine shape control, resulting in structurally well-defined electrocatalysts. Though hydrocarbon selectivity has recently been investigated on small Cu nanoparticles,[21–23] nanocubes,[24] and polyhedral with varying facets,[25] the general strategy of studying shape-controlled copper nanocatalysts is still underexplored.

One-dimensional nanowires (NWs) are an especially intriguing class of nanostructure for CO_2 electrocatalysis. The high density of low-coordination edge sites on a thin nanowire presents a catalytic surface with potential for high activity and unique selectivity, due to the difference in intermediate binding on low-coordinate sites. Zhu et al have previously shown markedly higher CO selectivity on ultrathin Au NWs, which they attribute by DFT calculations to enhanced intermediate binding on edge sites.[7] The catalytic influence of the NW morphology would be particularly interesting for Cu, due to its wider product distribution. Previous work on CO_2 reduction on Cu NWs have shown improved performance on wires with diameters ranging from 100 nm to several microns.[26–28] However, the catalytic activity of ultrathin Cu NWs, with a high density of well-defined twin boundaries, has yet to be investigated.

In the interest of investigating the morphological benefit of a high density of edge sites towards Cu-catalyzed CO_2 electroreduction, we studied the catalytic behavior of ultra-thin five-fold twinned Cu NWs, synthesized according to our previous report.[29] Figure 1a shows the

transmission electron microscope (TEM) images of the as-synthesized Cu NW with mean diameter of 17 nm. The wires have a five-fold-twinned structure as illustrated in the inset scheme. To test their catalytic behavior toward CO_2 reduction, freshly made Cu NWs were loaded onto carbon black (CB) with 20 wt% loading to make a CuNW/CB catalyst suspension in hexanes. TEM images of the composite catalyst confirmed the loading and contact of CuNWs with CB (Fig. 1c). This suspension was pasted onto glassy carbon plates to make the working electrode, which scanning electron microscopy (SEM) revealed to be a conductive network-like structure of Cu wires and carbon black (Fig. 1d). Direct loading of the Cu NW catalyst on the glassy carbon substrate was also explored. It was found that while the catalytic activities between the CuNW/GC and CuNW/CB/GC electrodes were comparable, the latter formulation was more mechanically stable. Without carbon black, the Cu NWs visibly disappeared from the electrode after 1 C of electrolysis (Fig S1).

Thereafter, the CuNW/CB catalyst was tested over a range of potentials for catalytic activity, showing a marked selectivity for methane among carbon products at potentials more negative than -1.1 V vs. RHE (Fig. 2a). Faradaic efficiencies (F.E.s) for methane at the potentials tested reached 55% at -1.25 V vs. RHE. Notably, while polycrystalline copper has frequently been reported to produce a spread of C1 and C2 products at potentials below -1 V vs. RHE, the CuNW catalyst produces nearly exclusively methane among the carbon-derived products. In fact, in the potential region tested spanning 600 mV, neither carbon monoxide (CO) nor ethylene (C_2H_4) exceed 5% of all products, while formate is only substantially produced at potentials more positive than -1 V vs. RHE. The Cu NW's high selectivity toward methane may be attributed to its high density of edge sites. The five twin boundaries on the ultra-thin wire present a unique active site for stabilizing CO_2 intermediates (Fig. 1b), which previous computation has also

suggested to enhance methane formation.[30] Total F.E.s consistently reached 90-100% at potentials where methane was produced selectively (Fig. 2b), suggesting the successful detection of all major products at methane-selective potentials.

To more aptly gauge the activity of the catalyst towards methane, the partial current density towards methane (j_{CH4}) was also calculated. For comparison, a polycrystalline copper foil electrode was measured under the same conditions, and the corresponding j_{CH4} values measured are within the range of previous results.[12,21] Although j_{CH4} for the two catalysts is comparable at lower overpotentials, the current of the CuNW-loaded electrode outpaces polycrystalline copper foil past -1.2 V vs. RHE (Fig. 2c). Control experiments showed that the background current from the same mass of carbon black on glassy carbon was minimal even at the most negative potentials applied (Fig. 2d), ruling out any contribution from the background carbon for these activities.

Electrocatalytic activity was also measured with varying amounts of passed charge before product measurement. Strikingly, the selectivity of the catalyst was observed to change with increasing charge passed at -1.25 V vs. RHE (Fig. 3a). Coulomb-by-Coulomb analysis of the activity evolution shows that the hydrocarbon selectivity shifts from almost complete CH_4 to higher C_2H_4 production over the course of 5 C passed. Other products (such as CO, H_2, and liquid products) were not observed to change substantially over this period (#S). The shift in selectivity appears shortly after the first Coulomb passed. This change in activity suggests a rapid evolution of the catalyst at potentials relevant to hydrocarbon formation. In parallel, the catalyst was observed to evolve morphologically over time. Figure 3b shows that after 1 C, the wire morphology begins to degrade, resulting in particle formation, wire bundling, disintegration, and fracturing. We posit that the evolution in electrocatalytic activity is strongly tied to the evolution

in morphology. Specifically, the loss of highly selective twin boundary edge sites results in a reduction in methane selectivity and a shift towards product distributions more closely resembling polycrystalline copper.

If the change in electrocatalytic activity were linked to a change in structure, then the selectivity should be preserved upon preserving structural features. Previous work on copper nanoparticles has shown a tendency for particles to sinter at high bias, potentially as a result of electrochemical migration or copper dissolution and redeposition.[21] One potential strategy for protecting the catalyst from this structural evolution is to surround it with a layer of material that impedes the nanoscale formation of copper nanoparticles, while retaining molecular scale diffusion of electrolyte and reactants to the catalyst surface. We have previously shown that these ultrathin copper nanowires can be wrapped with a thin reduced graphene oxide (rGO) shell to enhance structural stability.[31] To investigate whether the structure of a wire could be preserved, thereby also preserving the CO_2 electrocatalytic selectivity for methane, we studied the electrocatalytic properties of rGO-wrapped copper nanowires. rGO-wrapped wires were loaded on carbon black and glassy carbon under identical loading conditions to the bare Cu NWs and tested for CO_2 electrocatalytic activity.

Figure 3c shows the same set of experiments conducted on the rGO-CuNWs/CB catalyst. In contrast with the bare wires, rGO-wrapped wires preserve their selectivity for methane, as evidenced by the lack of a rise in ethylene. Simultaneously, the wires are observed to maintain their shape under TEM. Typical single wires were selected for Figure 3b and 3d to highlight the morphological difference between rGO-CuNWs and bare CuNWs under bias. TEM images of the ensemble nanowires for each catalyst imaged at varying points of the electrolysis have been included in the supplementary information (Fig. S#).

The result shown here aligns well with the idea that nanowire-specific structural features, such as edge sites, are responsible for stabilizing methane intermediates in CO_2 electroreduction, leading to heightened methane selectivity for five-fold twinned Cu NWs. As the wires evolve morphologically, the proportion of active sites described by twin boundaries decreases, while the proportion described by nanoparticles increases. The shift in selectivity for methane to ethylene shown here is approximately 10% F.E. Therefore, the final ethylene selectivity at -1.25 V vs. RHE is comparable to previous reports of ethylene selectivity for polycrystalline copper foil.[12] This evolved catalyst is ill-defined, with a diverse array of active sites consisting of roughened wires, small particles, and likely some remaining twin boundaries, and therefore exhibits mixed selectivity.

To verify that graphene oxide remains on the surface of the catalyst, we conducted Raman spectroscopy on the catalyst post-electrolysis. Fig. 4a shows the *D* and *G* bands corresponding to reduced graphene oxide,[32] which are present in the sample before testing and remains after 5 C of electrolysis. The qualitative weakening of the signal may be explained by the small amount of material used for post-electrolysis Raman, since the amount of material that can be recovered from a single electrode is low. For comparison, the unwrapped wires were also studied using Raman spectroscopy, and exhibited no peaks attributed to graphene oxide. To further reinforce that the graphene oxide wrapping is responsible for the preservation of selectivity, we varied the amount of graphene oxide used for wrapping the wires. Because the amount of graphene oxide wrapping originally used resulted in effectively no change in selectivity over 5 C, whereas no wrapping resulted in a shift of roughly 10%, we hypothesized that tuning the graphene oxide wrapping would result in intermediate shifts in selectivity. Energy dispersive X-ray spectroscopic (EDS) mapping verifies that graphene oxide is present around the

wires, and that increasing the mass ratio of graphene oxide to copper qualitatively increases the amount of graphene oxide wrapping (Fig 4b).

As shown in Fig. 4c, the amount of graphene oxide used correlates well with the methane selectivity over ethylene after 5C of electrolysis at -1.25 V vs. RHE, where methane selectivity can be better preserved with higher amounts of GO wrapping. The continued presence of graphene oxide on NWs that have neither evolved morphologically nor changed their selectivity, combined with the tunability of electrocatalytic selectivity with amount of graphene oxide, strongly confirms the role of graphene oxide in preserving structure and selectivity. Copper nanoparticle formation and edge loss shifts the morphology from high-density methane-selective sites to a mix of methane-selective and mixed-selectivity sites. Introducing graphene oxide as a wrapping layer impedes nanoscale structural change and prevents the loss of methane-selective sites (Fig. 4c).

In summary, we have shown that nanoscale one-dimensional five-fold twinned copper nanowires exhibit high methane selectivity for CO_2 electrocatalysis relative to other carbon products. We suggest that the origin of the methane selectivity is due to the presence of a high density of edge sites owing to the twin boundaries. Furthermore, we have demonstrated that on a short time scale, both the morphology of these wires and their electrocatalytic selectivity evolve, losing methane selectivity in favor of ethylene formation. We note that this time resolution is rarely investigated in previous literature, and that the morphological evolution can only be observed with spatial resolution of a few nm. We posit that the change in electrocatalytic selectivity is due to the change in morphology, specifically the loss of twin boundaries, and we support this claim by showing that wrapping the wires with graphene oxide preserves the morphology and simultaneously preserves methane selectivity. This study suggests a keen

relationship between nanoscale surface structure and CO_2 electrocatalytic selectivity on copper catalysts, a concept often discussed but rarely manipulated.

Associated content

Supporting Information Available: ## This material is available free of charge via the Internet at http://pubs.acs.org.

Author contributions

Y.L., F.C., and P. Y. designed the experiments and wrote the paper. F.C. and Y.S. synthesized copper nanowires and graphene oxide wrapped nanowires. Y.L. and F.C. carried out structural characterization. Y.L. and D.K. designed the electrochemical setup. Y.L. designed the electrode fabrication, carried out electrocatalytic tests, and quantified products with GC and NMR. M.B.R. conducted Raman spectroscopy on pre- and post-electrolysis samples. All authors discussed the results and commented on the manuscript.
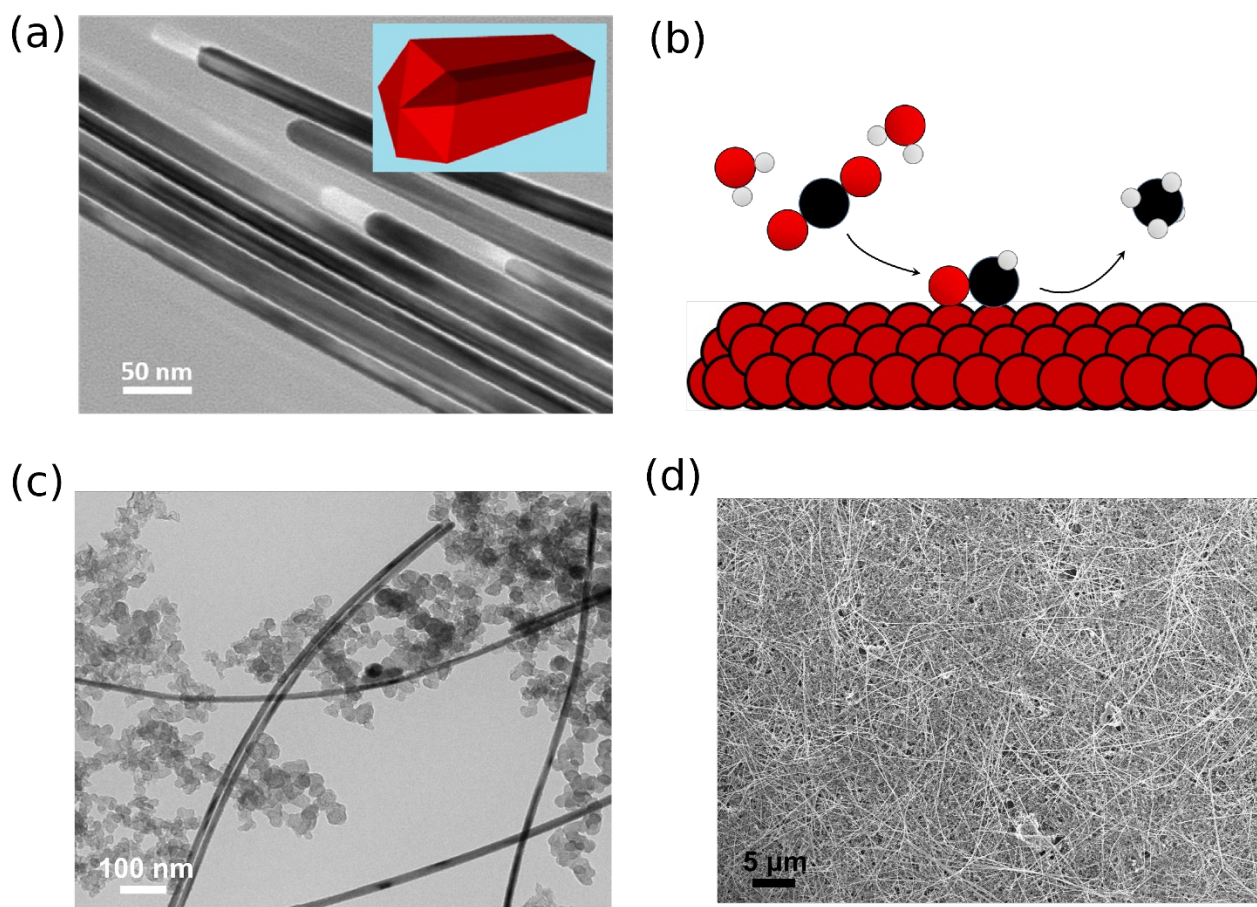
References

(1)   White, J. L.; Baruch, M. F.; Pander, J. E.; Hu, Y.; Fortmeyer, I. C.; Park, J. E.; Zhang, T.; Liao, K.; Gu, J.; Yan, Y.; Shaw, T. W.; Abelev, E.; Bocarsly, A. B. *Chem. Rev.* **2015**, *115* (23), 12888–12935.

(2)   Kim, D.; Sakimoto, K. K.; Hong, D.; Yang, P. *Angew. Chemie - Int. Ed.* **2015**, *54* (11), 3259–3266.

(3)   Kondratenko, E. V; Mul, G.; Baltrusaitis, J.; Larrazabal, G. O.; Perez-Ramirez, J. *Energy Environ. Sci.* **2013**, *6* (11), 3112.

(4)   Rosen, B. A.; Salehi-Khojin, A.; Thorson, M. R.; Zhu, W.; Whipple, D. T.; Kenis, P. J. A.; Masel, R. I. *Science* **2011**, *334* (6056), 643–644.

(5)   Lu, Q.; Rosen, J.; Zhou, Y.; Hutchings, G. S.; Kimmel, Y. C.; Chen, J. G.; Jiao, F. *Nat. Commun.* **2014**, *5*, 3242.

(6)   Kim, D.; Resasco, J.; Yu, Y.; Asiri, A. M.; Yang, P. *Nat. Commun.* **2014**, *5*, 4948.

(7)   Zhu, W.; Zhang, Y. J.; Zhang, H.; Lv, H.; Li, Q.; Michalsky, R.; Peterson, A. A.; Sun, S. *J. Am. Chem. Soc.* **2014**, *136* (46), 16132–16135.

(8)   Chen, Y.; Li, C. W.; Kanan, M. W. *J. Am. Chem. Soc.* **2012**, *134* (49), 19969–19972.

(9)   Liu, M.; Pang, Y.; Zhang, B.; De Luna, P.; Voznyy, O.; Xu, J.; Zheng, X.; Dinh, C. T.; Fan, F.; Cao, C.; de Arquer, F. P. G.; Safaei, T. S.; Mepham, A.; Klinkova, A.; Kumacheva, E.; Filleter, T.; Sinton, D.; Kelley, S. O.; Sargent, E. H. *Nature* **2016**, *537* (7620), 382–386.

(10)   Kuhl, K. P.; Hatsukade, T.; Cave, E. R.; Abram, D. N.; Kibsgaard, J.; Jaramillo, T. F. *J. Am. Chem. Soc.* **2014**, *136* (40), 14107–14113.

(11)   Hori, Y. In *Modern Aspects of Electrochemistry*; 2008; pp 89–189.

(12)   Kuhl, K. P.; Cave, E. R.; Abram, D. N.; Jaramillo, T. F. *Energy Environ. Sci.* **2012**, *5* (5), 7050.

(13)   Gattrell, M.; Gupta, N.; Co, A. *J. Electroanal. Chem.* **2006**, *594* (1), 1–19.

(14)   Tang, W.; Peterson, A. A.; Varela, A. S.; Jovanov, Z. P.; Bech, L.; Durand, W. J.; Dahl, S.; Nørskov, J. K.; Chorkendorff, I. *Phys. Chem. Chem. Phys.* **2012**, *14* (1), 76–81.

(15)   Zhang, S.; Kang, P.; Meyer, T. J. *J. Am. Chem. Soc.* **2014**, *136* (5), 1734–1737.

(16)   Li, C. W.; Kanan, M. W. *J. Am. Chem. Soc.* **2012**, *134* (17), 7231–7234.

(17)   Kas, R.; Kortlever, R.; Yılmaz, H.; Koper, M. T. M.; Mul, G. *ChemElectroChem* **2015**, *2* (3), 354–358.

(18)   Ren, D.; Deng, Y.; Handoko, A. D.; Chen, C. S.; Malkhandi, S.; Yeo, B. S. *ACS Catal.* **2015**, *5* (5), 2814–2821.
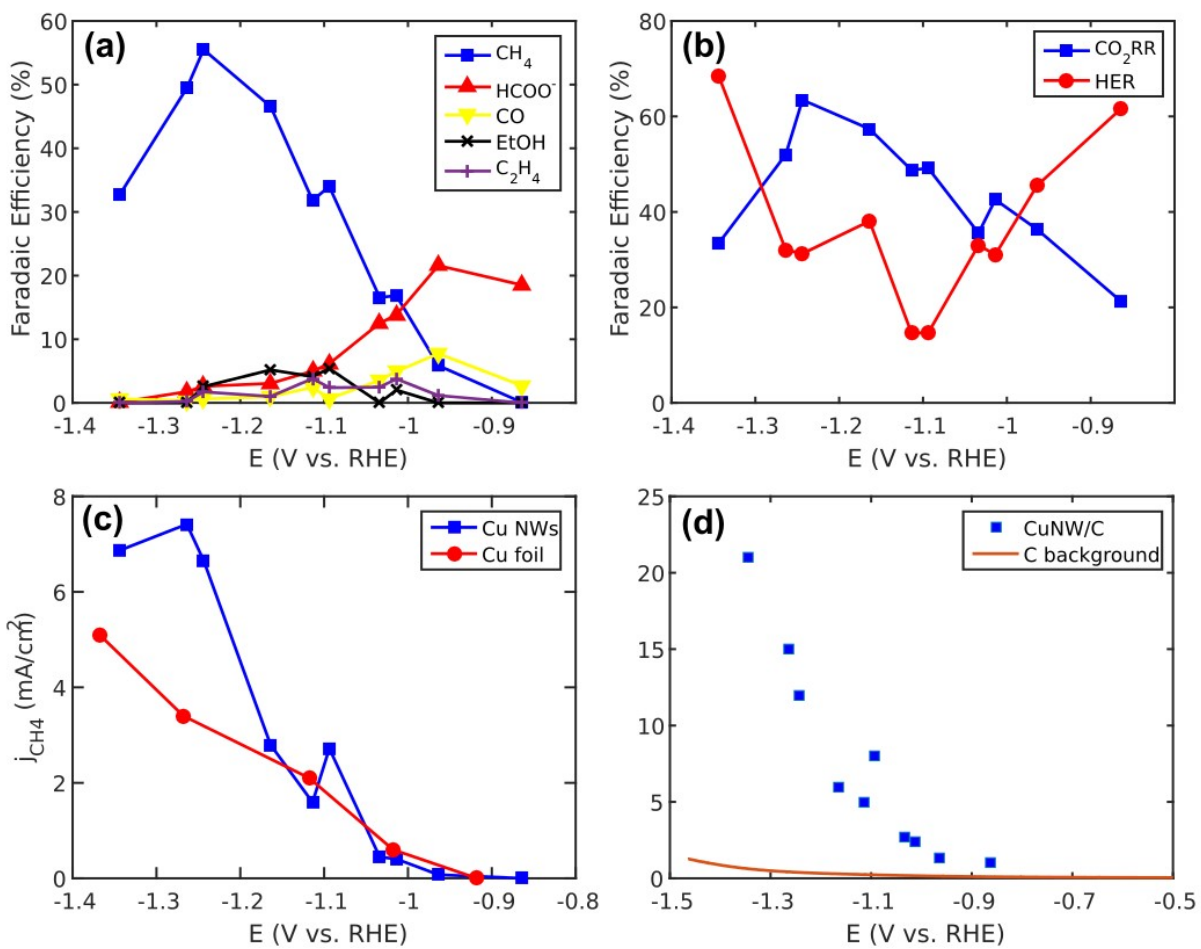
(19)   Roberts, F. S.; Kuhl, K. P.; Nilsson, A. *Angew. Chemie* **2015**, n/a – n/a.

(20)   Mistry, H.; Varela, A. S.; Bonifacio, C. S.; Zegkinoglou, I.; Sinev, I.; Choi, Y.; Kisslinger, K.; Stach, E. A.; Yang, J. C.; Strasser, P.; Cuenya, B. R. *Nat. Commun.* **2016**, *7* (12123), 1–8.

(21)   Manthiram, K.; Beberwyck, B. J.; Alivisatos, A. P. *J. Am. Chem. Soc.* **2014**, *136* (38), 13319–13325.

(22)   Baturina, O. A.; Lu, Q.; Padilla, M. A.; Xin, L.; Li, W.; Serov, A.; Artyushkova, K.; Atanassov, P.; Xu, F.; Epshteyn, A.; Brintlinger, T.; Schuette, M.; Collins, G. E. *ACS Catal.* **2014**, *4* (10), 3682–3695.

(23)   Reske, R.; Mistry, H.; Behafarid, F.; Roldan Cuenya, B.; Strasser, P. *J. Am. Chem. Soc.* **2014**, *136* (19), 6978–6986.

(24)   Loiudice, A.; Lobaccaro, P.; Kamali, E. A.; Thao, T.; Huang, B. H.; Ager, J. W.; Buonsanti, R. *Angew. Chemie - Int. Ed.* **2016**, *55* (19), 5789–5792.

(25)   Wang, Z.; Yang, G.; Zhang, Z.; Jin, M.; Yin, Y. *ACS Nano* **2016**, acsnano.6b00602.

(26)   Ma, M.; Djanashvili, K.; Smith, W. A. *Angewandte Chemie - International Edition*. June 1, 2016, pp 6680–6684.

(27)   Raciti, D.; Livi, K. J.; Wang, C. *Nano Lett.* **2015**, *15* (10), 6829–6835.

(28)   Xie, M. S.; Xia, B. Y.; Li, Y.; Yan, Y.; Yang, Y.; Sun, Q.; Chan, S. H.; Fisher, A.; Wang, X. *Energy Environ. Sci.* **2016**, *9*, 1687–1695.

(29)   Cui, F.; Yu, Y.; Dou, L.; Sun, J.; Yang, Q.; Schildknecht, C.; Schierle-Arndt, K.; Yang, P. *Nano Lett.* **2015**, *15* (11), 7610–7615.

(30)   Chen, Z.; Zhang, X.; Lu, G. *Chem. Sci.* **2015**, *6* (2), 6829–6835.

(31)   Dou, L.; Cui, F.; Yu, Y.; Khanarian, G.; Eaton, S. W.; Yang, Q.; Resasco, J.; Schildknecht, C.; Schierle-Arndt, K.; Yang, P. *ACS Nano* **2016**, *10* (2), 2600–2606.

(32)   Stankovich, S.; Dikin, D. A.; Piner, R. D.; Kohlhaas, K. A.; Kleinhammes, A.; Jia, Y.; Wu, Y.; Nguyen, S. T.; Ruoff, R. S. *Carbon N. Y.* **2007**, *45* (7), 1558–1565.
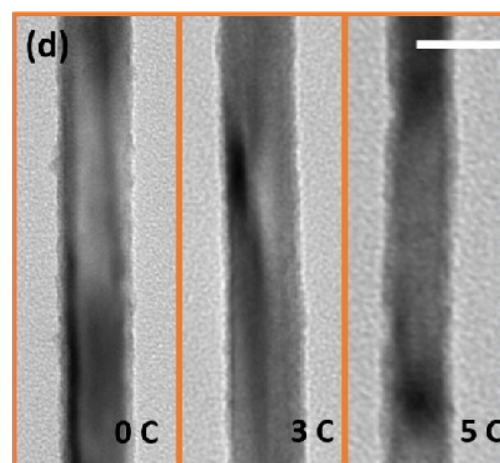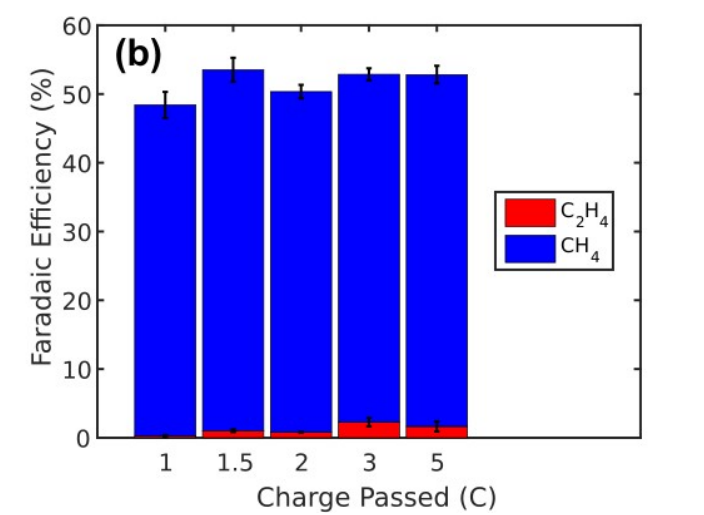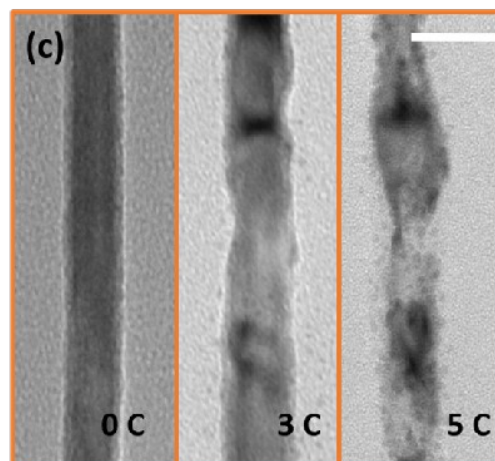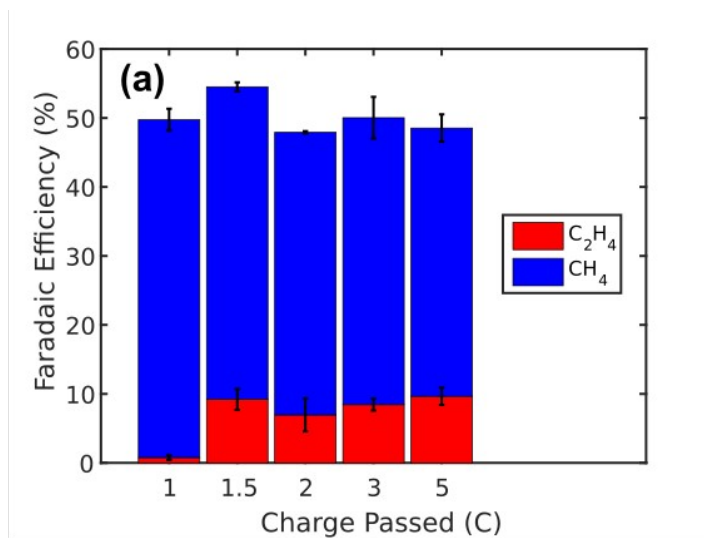
Figures

Figure 1

(a)

(b)

(c)

(d)

Figure 2

Figure 3

Figure 4

(a) D G rGO-CuNW, 5 C

rGO-CuNW, 0 C

bare CuNW

Normalized Intensity

1200 1400 1600 1800 2000 2200
Raman Shift (cm^{-1})

(b)

0.0062   0.012   0.025   0.05   0.1

C Cu

(c)

F.E. @ 5C (%)

60
50
40
30
20
10
0

CH_4

C_2H_4

0   0.02   0.04   0.06   0.08   0.1
rGO-Cu Mass Ratio

(d)

Formation of Cu NPs

Preservation of Cu NW morphology
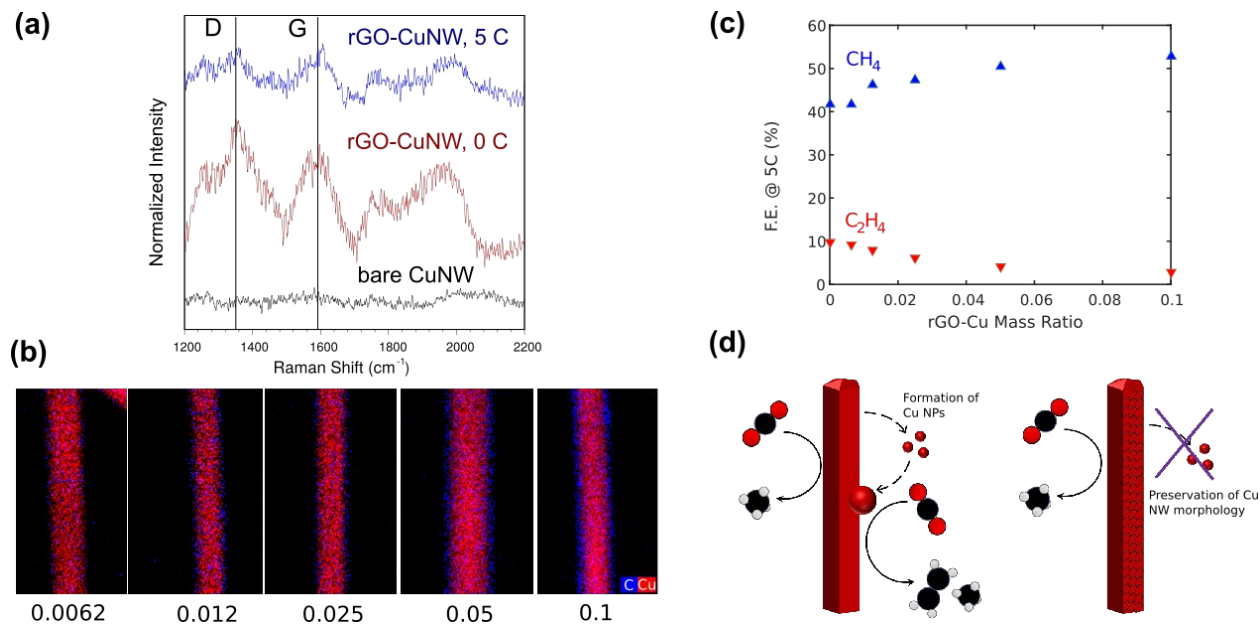
Figure captions

Figure 1: Synthesis of five-fold twinned copper nanowires. (a) TEM image of bare wires, around

20 nm in diameter, before loading. Inset: illustration of a high proportion of low-coordination

edge sites brought about by five-fold twin boundaries. (b) Illustration of CO_2 electroreduction to

methane with a stabilized intermediate bound by Cu NW edge sites. (c) TEM image of Cu NWs

loaded on carbon black with 20 wt% loading. (d) SEM image of the CuNW/CB catalyst

dispersed on a glassy carbon surface, used as the electrode for electrochemical experiments.

Figure 2: Cu NW electrocatalytic activity and selectivity over the potential range of -0.85 to -

1.35 V vs. RHE in 0.1 M $KHCO_3$ over 1 C of passed charge. (a) Products of CO_2 reduction,

showing the prevalence of CH_4 at high bias over other products (CO, C_2H_4, formate, and

ethanol). Acetate, methanol, and n-propanol were detected in trace. (b) Total F.E. of CO_2RR and

the competing reaction, hydrogen evolution. (c) Partial current density towards methane of the

Cu NW catalyst compared with a cleaned polycrystalline copper foil, showing the increased

activity at more negative potential. (d) Total geometric current density over the range of potentials, compared to background current from the glassy carbon substrate with bare carbon black loaded.

Figure 3: Parallel electrocatalytic and morphological evolution of the Cu NW catalyst. (a) Rapid onset of C_2H_4 formation after the first Coulomb of electrolysis, matched with a decrease in CH_4 activity. (b) Representative Cu NWs imaged under TEM after a given amount of charge passed, showing visible fracturing and the formation of small Cu NPs. (c), (d) Analogous electrocatalytic and morphological characterization for the rGO-Cu NW catalyst, showing preservation in both domains. Scale bar for TEM: 50 nm.

Figure 4: Evidence for the protective role of reduced graphene oxide. (a) From bottom to top, Raman spectra of bare CuNWs, GO-wrapped CuNWs before electrolysis, and GO-wrapped CuNWs after electrolysis. The D and G peaks attributable to graphene oxide are indicated, showing its presence and retention after 5 C electrolysis. (b) EDS mapping of GO-wrapped CuNWs with varying amounts of GO, showing the increasing presence of carbon species attributed to graphene oxide surrounding the wires. (c) CH_4 and C_2H_4 selectivity at 5 C on Cu NWs wrapped with varying amounts of GO, showing preservation of CH_4 selectivity with increasing GO wrapping. (d) Scheme for the correlation between morphology and selectivity observed in this study. C_2H_4 onset is thought to be due to the transformation of NW edge sites to small NPs deposited on the surface (left), which GO wrapping prevents (right).